

enol ether product **2** with the observed atropselectivity.

In summary, Smith and co-workers have demonstrated an elegant new approach for the organocatalyzed asymmetric synthesis of axially chiral biaryls. The chiral ammonium counterion differentiates between rapidly equilibrating atropisomeric enolates to give an axially chiral enol ether product with high enantioselectivity. This interesting asymmetric approach for the synthesis of axially chiral com-

pounds offers new insight into the catalytic asymmetric synthesis of important chiral compounds.

1. Bringmann, G., Price Mortimer, A.J., Keller, P.A., Gresser, M.J., Garner, J., and Breuning, M. (2005). *Angew. Chem. Int. Ed. Engl.* **44**, 5384–5427.
2. Wencel-Delord, J., Panossian, A., Leroux, F.R., and Colobert, F. (2015). *Chem. Soc. Rev.* **44**, 3418–3430.
3. Bencivenni, G. (2015). *Synlett* **26**, 1915–1922.
4. Shirakawa, S., Liu, S., and Kaneko, S. (2016). *Chem. Asian J.* **11**, 330–341.
5. Shirakawa, S., and Maruoka, K. (2013). *Angew. Chem. Int. Ed. Engl.* **52**, 4312–4348.
6. Shirakawa, S., Wu, X., and Maruoka, K. (2013). *Angew. Chem. Int. Ed. Engl.* **52**, 14200–14203.
7. Shirakawa, S., Wu, X., Liu, S., and Maruoka, K. (2016). *Tetrahedron* **72**, 5163–5171.
8. Armstrong, R.J., and Smith, M.D. (2014). *Angew. Chem. Int. Ed. Engl.* **53**, 12822–12826.
9. Jolliffe, J.D., Armstrong, R.J., and Smith, M.D. (2017). *Nat. Chem.* Published online January 23, 2017. <http://dx.doi.org/10.1038/nchem.2710>.
10. Kano, T., Hayashi, Y., and Maruoka, K. (2013). *J. Am. Chem. Soc.* **135**, 7134–7137.

## Preview

# STED Nanoscopy Goes Low Power

Liangliang Liang<sup>1</sup> and Xiaogang Liu<sup>1,2,\*</sup>

**An extremely high depletion intensity is a general prerequisite for achieving high-resolution STED (stimulated emission depletion) nanoscopy. In a recent paper published in *Nature*, Liu et al. devised lanthanide-doped upconversion nanoparticles as luminescent probes for STED nanoscopy with an ultralow-power laser depletion beam.**

Far-field fluorescence microscopy has become a versatile tool for investigating biological specimens non-invasively and enabling spectroscopic analysis with unparalleled chemical sensitivity. But the weakness of this optical method has always been its diffraction-limited spatial resolution. Although new imaging techniques such as atomic force microscopy can defy the diffraction limit of light and provide nanoscale visualization, they are surface bound and incapable of assessing the dynamic structural changes that occur inside the biological specimens.

The path to far-field fluorescence microscopy with sub-diffraction resolution

was enlightened by the ingenious proposal of Stefan W. Hell, who believed that stimulated emission depletion (STED) fluorescence microscopy would help to break the diffraction barrier.<sup>1</sup> Most implementations of this concept involve the use of a focused excitation beam superimposed by a doughnut-shaped STED beam that instantly depletes excited fluorophores to dim the overlapping area. This process results in a fluorescence spot far below the diffraction limit, making it possible to achieve super-resolution imaging.<sup>2,3</sup>

Raising the intensity of the de-excitation beam is likely to suppress the fluorescent region of the given fluoro-

phores more efficiently, leading to a shrunken spot around the zero-intensity point and thus improved imaging resolution. Indeed, constrained by the ultrafast spontaneous emission nature of commonly used fluorophores, such as organic molecules and quantum dots,<sup>2,4,5</sup> STED beams with extremely high power densities are indispensable for achieving the maximum depletion efficiency. However, aggravated fluorophore photobleaching and irreparable damage of biological samples, triggered by the high-power beam, inevitably deprive STED nanoscopy of many application opportunities, especially in extended time-lapse imaging. In a recent publication in *Nature*, Dayong Jin at the University of Technology Sydney, Peng Xi at Peking University, and their colleagues report a new approach that offers a substantial reduction in the threshold for STED beam intensity to realize super-resolved STED nanoscopy.<sup>6</sup>

<sup>1</sup>Department of Chemistry, National University of Singapore, Singapore 117543, Singapore

<sup>2</sup>Institute of Materials Research and Engineering, Singapore 117602, Singapore

\*Correspondence: [chmlx@nus.edu.sg](mailto:chmlx@nus.edu.sg)

<http://dx.doi.org/10.1016/j.chempr.2017.02.016>

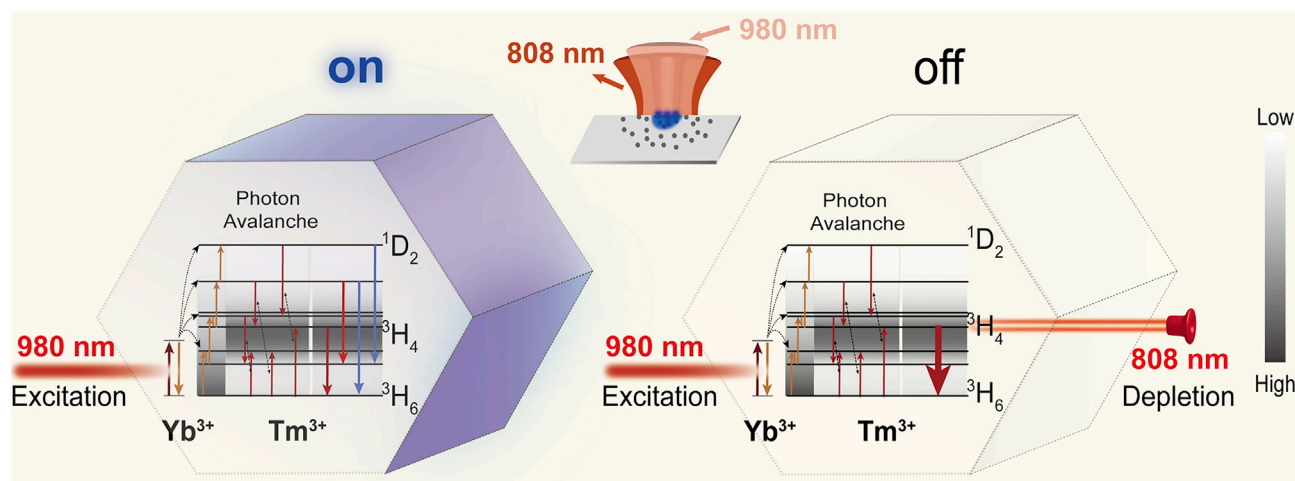


**Figure 1. Photon-Avalanche-Mediated STED in Upconversion Nanoparticles Highly Doped with  $\text{Tm}^{3+}$**

Schematic showing the effect of the combined action of 980 nm excitation and 808 nm depletion on upconversion luminescence. A high doping concentration of activators leads to drastically shortened distance and thus strong cross-relaxation between neighboring  $\text{Tm}^{3+}$  ions, resulting in photon avalanche and population inversion between the  $^3\text{H}_4$  and  $^3\text{H}_6$  states. Therefore, the amplified stimulated emission caused by the 808 nm beam can deplete the  $^3\text{H}_4$  state and switch off the upconversion emission efficiently. (The plot legend schematically refers to the population density of the  $\text{Tm}^{3+}$  activator.)

The key element of the approach is designing thulium-doped upconversion nanoparticles ( $\text{NaYF}_4$ : 20% Yb and 8% Tm) as the luminescent probe. These nanoparticles are capable of emitting a photon at a shorter wavelength after absorbing two or more photons of longer wavelengths.<sup>7</sup> Benefitting from their innate advantages, such as high photostability, long lifetime, and superior biocompatibility, upconversion nanoparticles are promising for STED nanoscopic applications. However, to overcome the problem of luminescence-concentration quenching induced by cross-relaxation, a relatively low concentration of activators, typically less than 2 mol %, is usually adopted,<sup>8</sup> rendering an excited-state population nature similar to that of organic dyes or quantum dots. Consequently, a high-power beam is still required for maximizing the optical de-excitation by stimulated emission.

Inspired by the fundamental working principle of lasers,<sup>9</sup> Jin and colleagues have now succeeded in bringing down the depletion-intensity threshold for

STED nanoscopy by utilizing a photon avalanche in nanoparticles with heavily doped  $\text{Tm}^{3+}$  ions. They showed that for nanoparticles with 8 mol % of  $\text{Tm}^{3+}$  dopants, the visible emission of  $\text{Tm}^{3+}$  upon excitation with a continuous-wave 980 nm laser could be visibly counteracted once an 808 nm de-excitation beam was applied. In contrast, samples doped with a low concentration of  $\text{Tm}^{3+}$  ions (1 mol %) showed negligible changes in the emission profile. Furthermore, the researchers found that as the dopant content increased, the saturation intensity required for halving the original emission dropped sharply to  $\sim 0.19 \text{ MW/cm}^2$ , which is almost 2 orders of magnitude lower than that achievable by previously developed STED techniques. This design allows for super-resolution imaging with a lateral resolution of 28 nm to be achieved under a low-power density field ( $9.75 \text{ MW/cm}^2$ ). Apparently, all available evidence points to the fact that the doping concentration of  $\text{Tm}^{3+}$  plays a crucial role in dictating the performance of upconversion nanoparticle STED. But what is the mechanism underlying this concentration-dependent optical phenomenon?

The rate of energy transfer between adjacent lanthanide ions can be facilitated by an increase in the doping concentration.<sup>10</sup> For example, a  $\text{Tm}^{3+}$  ion in its  $^1\text{D}_2$  excited state can transfer part of its energy to a neighboring ground-state  $\text{Tm}^{3+}$  ion in a process known as cross-relaxation, allowing both ions to occupy the intermediate  $^3\text{H}_4$  level. At a high doping concentration of  $\text{Tm}^{3+}$ , cross-relaxation dominates the optical process because of the short Tm-Tm distance. This can trigger a photon avalanche, a unique upconversion mechanism whereby the intermediate excited energy levels can be rapidly populated to establish a population inversion between metastable level  $^3\text{H}_4$  and ground level  $^3\text{H}_6$ . In that respect, upon 808 nm beam depletion, amplified stimulated emission is possible, resulting in a higher depletion efficiency and thus a reduced saturation intensity (Figure 1).

To confirm the photon avalanche in nanoparticles with high  $\text{Tm}^{3+}$  dopant content, Jin and colleagues recorded transient emission at 800 nm from the  $^3\text{H}_4$  level of  $\text{Tm}^{3+}$  under 980 nm

excitation. The steep “S” shape build-up curve provided concrete supporting evidence for the occurrence of the photon avalanche process. Additionally, the authors showed that for nanoparticles doped with 1 mol % of  $\text{Tm}^{3+}$ , the 808 nm beam could promote (instead of deplete) the population of the  $^3\text{H}_4$  level and enhance upconversion emission, indicating the decisive role of high doping concentration of  $\text{Tm}^{3+}$  in triggering the avalanche process.

The discovery of highly lanthanide-doped upconversion nanoparticles suitable for STED nanoscopy is encouraging because it provides a feasible way to achieve super-resolution with a low-power-density depletion beam. As such, the issue of photothermal damage, typically associated with high-power-density beams, to biological samples can be effectively addressed. Given the high photostability and non-blinking characteristics of upconversion nanoparticles, a particularly attractive application of these nanoparticles and STED nanoscopy would appear to be

time-lapse imaging of living biological specimens.

The hot question coming out of such an impressive experiment is its performance and suitability when applied in real biological settings under physiological conditions. Unfortunately, the forbidden nature of 4f-4f transition of lanthanides can severely slow down the rate of upconversion emission, resulting in a drastically prolonged dwell time and imaging acquisition time. The necessity for the lengthy data collection and processing would most likely compromise the practicability of these nanoprobe for wide STED nanoscopic applications. As it happens, the continuity in the time lapse recorded with repeated frames will be broken down because it is unrealistic to capture each frame for imaging large-area specimens. In addition, the imaging resolution of this technique is limited by the size of the nanoparticles in use. To further push the spatial resolution limit, one has to consider the preparation of high-efficiency upconversion nanoparticles smaller than

10 nm, a challenging size regime where significant surface quenching of upconversion luminescence becomes an issue.

1. Hell, S.W., and Wichmann, J. (1994). *Opt. Lett.* 19, 780–782.
2. Klar, T.A., and Hell, S.W. (1999). *Opt. Lett.* 24, 954–956.
3. Hell, S.W. (2007). *Science* 316, 1153–1158.
4. Resch-Genger, U., Grabolle, M., Cavaliere-Jaricot, S., Nitschke, R., and Nann, T. (2008). *Nat. Methods* 5, 763–775.
5. Hanne, J., Falk, H.J., Görlitz, F., Hoyer, P., Engelhardt, J., Sahl, S.J., and Hell, S.W. (2015). *Nat. Commun.* 6, 7127.
6. Liu, Y., Lu, Y., Yang, X., Zheng, X., Wen, S., Wang, F., Vidal, X., Zhao, J., Liu, D., Zhou, Z., et al. (2017). *Nature*. Published online February 22, 2017. <http://dx.doi.org/10.1038/nature21366>.
7. Auzel, F. (2004). *Chem. Rev.* 104, 139–173.
8. Yin, A., Zhang, Y., Sun, L., and Yan, C. (2010). *Nanoscale* 2, 953–959.
9. Stoneman, R.C., and Esterowitz, L. (1990). *Opt. Lett.* 15, 486–488.
10. Deng, R., Wang, J., Chen, R., Huang, W., and Liu, X. (2016). *J. Am. Chem. Soc.* 138, 15972–15979.